

EXPERIMENTAL STUDY ON A TWO-DIMENSIONAL FLUID-STRUCTURE INTERACTION REFERENCE TEST CASE

Hermann Lienhart, Jorge Pereira Gomes

Lehrstuhl für Strömungsmechanik, Universität Erlangen-Nürnberg
Cauerstraße 4, D-91058 Erlangen, Germany
e-mail: lienhart@lstm.uni-erlangen.de
jgomes@lstm.uni-erlangen.de
Web page: <http://lstm.uni-erlangen.de/>

Key words: Fluid-Structure interaction, Particle image velocimetry, laminar reference experiment.

Abstract. *Experimental studies on reference test cases are of capital importance to support the development of models and coupling strategies for simulations on fluid-structure interaction problems. The need for experimental test cases specially addressed for the validation and diagnostic of numerical tools has triggered the present contribution to design and to study two-dimensional reference test cases both in laminar and turbulent flows.*

From the experimental view point, investigations on coupled unsteady flow and structure motions require specially adapted test rigs and measuring techniques to obtain accurate time-phase resolved results. Therefore a new experimental facility to be operated with a large range of viscous liquids was built exclusively for the present study. It made possible to perform measurements, using optical laser measurement techniques, in laminar and turbulent flows under very well controlled boundary and working conditions. A Particle Image Velocimetry (PIV) measuring system was adapted to measure both the periodical flow velocity field and the structure deflection modes.

The first reference test cases were conducted in laminar flows (Reynolds number ≤ 200). In that period an extended investigation was performed on the coupled motion of relatively simple two-dimensional reference structures immersed in a high viscous fluid (kinematic viscosity of $0,000164 \text{ m}^2/\text{s}$). This paper presents a complete characterization of a reference test case for an incoming velocity of $1,45 \text{ m/s}$.

1 INTRODUCTION

Flow-structure interaction problems, involving the coupling of unsteady fluid flow and structure motion, arise in many fields of engineering^{1,2} as well as in many other sciences, e.g. medicine. From previous experience one can conclude that the mechanisms which lead the vibration of flexible structures immersed in flowing fluids to become self-excited are very sensitive to the mechanical properties of the structure as well as to the properties of the incoming fluid and very difficult to predict.

With the continuous increase of computer power, these problems have attracted more and more interest of the computational mechanics. However, in spite of the practical relevance of the prediction of coupled fluid and structural dynamics in many technical problems, this type

of simulation is not yet considered a validated tool. Increased efforts in numerical research and development are presently being observed to develop models and coupling strategies for numerical simulations and to create coupling algorithms between computational fluid dynamics (CFD) and computational structural dynamics (CSD) solvers.

A group of University institutes has decided to form a research group to work on this subject. This common effort shall result in new tools which permit a realistic simulation of such complex, nonlinear coupled problems. However, to ensure success, comparisons with experimental studies are needed. This demand has triggered the present contribution to perform a reference experiment specially dedicated toward the diagnostic and validation of the numerical models for fluid-structure interaction simulations. The main objective was to establish a common experimental test case on fluid-structure interaction and to provide a reliable data base to serve the validation and comparison purposes of the different numerical methods and codes implementations.

The firsts test cases preformed were focused in the laminar regime with a Reynolds number limited up to 500. These experiments were carried out in incompressible high viscous fluids. Later additional tests were performed in water to extend the study to turbulent flows. The data base created on these reference test cases includes the time-phase resolved information about the flow velocity field and the mechanical behavior of the structure such as its deflection, principal deflection modes, periodical motion amplitude and frequency.

The present paper exclusively refers to the laminar reference test case.

2 EXPERIMENT DEFINITION

The experiment aimed to characterize the resulting two-dimensional periodical swiveling motion of relatively simple flexible structures driven by a constant incoming laminar fluid flow. The requirements of the tests imposed stringent restrictions to the selection of the reference structure and to the definition of the test conditions.

The final choice of the structure geometry to be studied in full detail took into account five principal aspects: (i) reproducibility of the resulting motion, (ii) two-dimensionality of the structure deflection, (iii) moderate structure motion frequency and (iv) significant excursion of the structure (v) well defined linear mechanical proprieties of the structure.

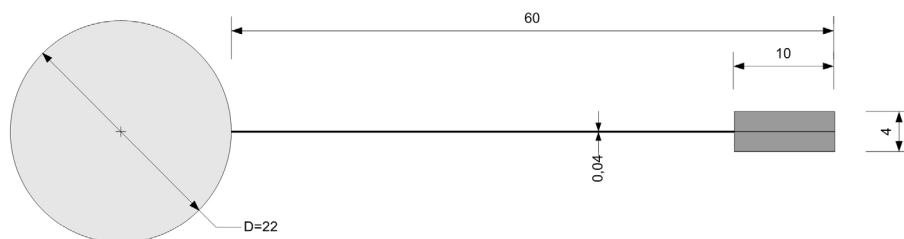


Fig. 1. Structure layout (all dimensions in mm).

After a period of preliminary tests the structure was defined to be constituted by a 0,04 mm thick stainless steel sheet attached to an 22 mm diameter aluminum cylindrical front body (see Fig. 1). At the trailing edge of the membrane a 10 mm × 4 mm rectangular stainless steel mass was located. All the structure was free to rotate around an axle located in the center point of the front cylinder. Both the front cylinder and the rear mass were considered rigid. The flexible section of the structure has proven to show a linear mechanical behavior within the range of forces acting on it during the tests and the Young modulus was measured to be 200 kN/mm². The overall spanwise dimension of the structure was 177 mm.

The structure was mounted 55 mm downstream the inlet plane of the 338 mm long test section on ball bearings, therefore, the rotational degree of freedom of the front cylinder could be considered to be free of friction. The experiment domain of the reference experiment is represented in figure 2.

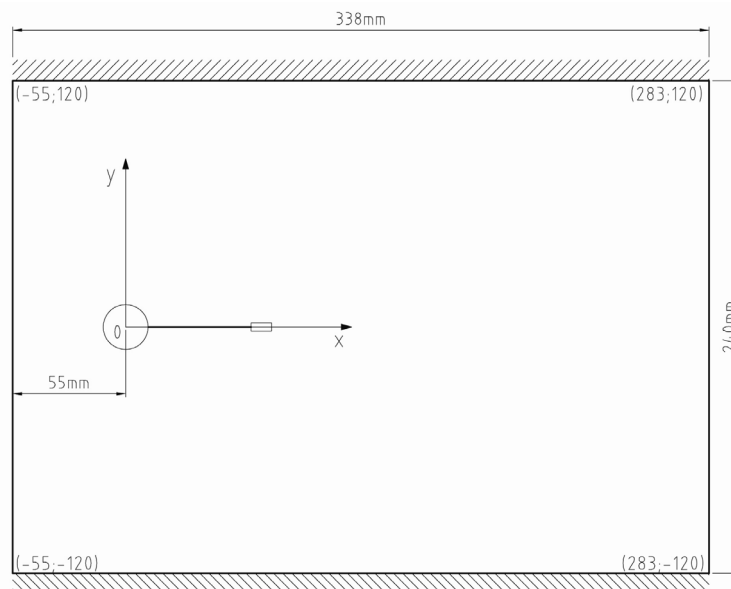


Fig. 2. Experiment domain.

The tests at low Reynolds number were conducted using polyethylene glycol PG-12000 syrup as the test fluid. The mixture could be considered incompressible and was prepared in such a way that the kinematic viscosity and the density of the fluid were equal to 0,000164 m²/s and 1050 kg/m³, respectively.

3 EXPERIMENTAL APPARATUS

3.1 FLUSTRUC experimental facility

To provide the details needed for numerical validation and accuracy verification purposes the test cases had to be conducted under very precise and controllable boundary and working conditions. This requirement and the necessity of very low Reynolds numbers determined the

construction of a new facility especially dedicated to fluid-structure interaction studies. It is a vertical closed circuit tunnel powered by a 24kW axial propeller pump (see Fig. 3). Its was designed to have a kinematic viscosity operation range from $1 \times 10^{-6} \text{ m}^2/\text{s}$ up to $5 \times 10^{-4} \text{ m}^2/\text{s}$. The facility is capable to maintain a constant maximum flow velocity in the test section of about 4,5 m/s and 2,7 m/s, when operated with water as working fluid or a $0,000164 \text{ m}^2/\text{s}$ kinematic viscosity liquid fluid, respectively.

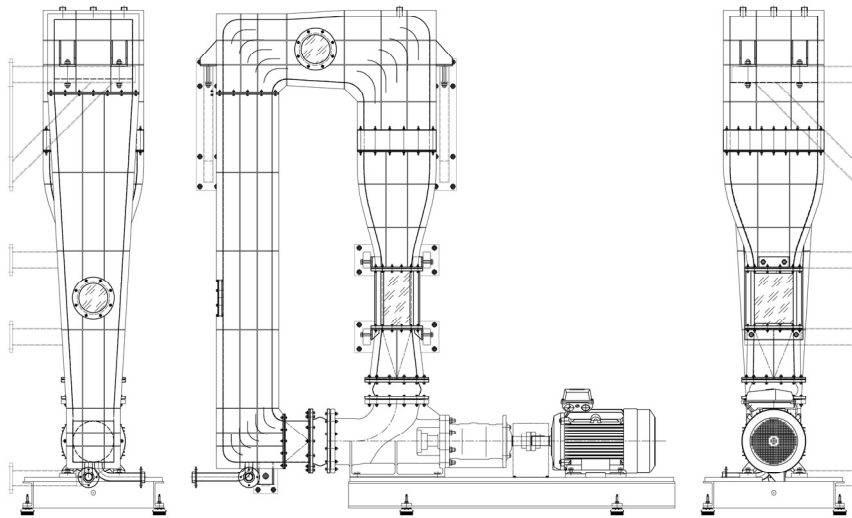


Fig. 3. FLUSTRUC tunnel layout.

Strong emphasis was placed on the design of the $180 \text{ mm} \times 240 \text{ mm}$ cross section, 338 mm long test section to allow flow investigation using laser measurement techniques (specially PIV and LDA). The model was mounted between two opposite walls on low friction bearings 55 mm downstream of the test section inlet. The gravity force is aligned with the x-axis and so it does not introduce any asymmetry.

To control the viscosity of the working liquid Polyethylene Glycol (Polyglycol) PG-12000 syrups were used. They permitted an accurate control of the kinematic viscosity of the tests within the operation range of the facility. From a kinematic viscosity of $1 \times 10^{-6} \text{ m}^2/\text{s}$ up to $5 \times 10^{-4} \text{ m}^2/\text{s}$ the density of the Polyglycol syrups exhibit a minor variation of 10% in respect to water.

3.2 Time-phase resolved measurements

When investigating periodical fluid-structure interaction problems two additional difficulties appear when it comes to resolve the measured data in time-phase space. Firstly, the periodicity of the structure motion is quite sensitive to the flow conditions and structure mechanical properties; therefore, there are cycle-to-cycle variations of the period time. Secondly, the velocity of the structure within a motion period is not predefined (as it is for

crank shaft driven set-ups) which makes it impossible to reconstruct the time-phase resolved data from position resolved measurements. Because of this it was decided not to trigger the data acquisition by the experiment and to implement a different time-phase resolving system.

In the present approach the measuring system was operated at constant acquisition rate and both events, the acquisition of a measurement and the start of a new cycle of the structure motion were recorded based upon an absolute clock. Using the recorded events time information the data was reorganized in a post-processing software in order to generate the time-phase resolved data. Besides solving the trigger problem, this solution also resulted in a minimum acquisition time needed, because the measuring system could be always operated at its optimum measuring rate independent of the structure swiveling frequency.

To execute this idea a time-phase detector module was designed to perform the event monitoring and integrated in the measuring system. The hardware module is based on a FPGA (Field Programmable Gate Array) and a 1 MHz internal clock. It is capable to monitor up to 250 events per second from 6 different lines with an accuracy of 2 μ s.

$$T_i = t_{i+1} - t_i \quad (1)$$

$$t_j = \frac{t_{ij} - t_i}{T_i} \times 360^\circ \quad (2)$$

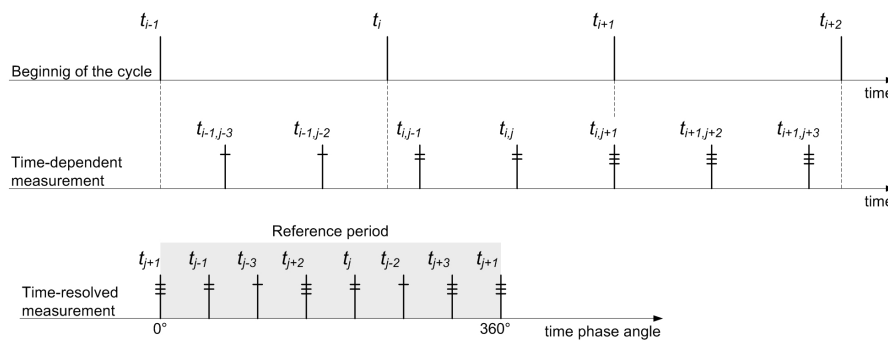


Fig. 4. Time-phase measurements reconstruction time scheme.

Figure 4 shows a typical time-phase resolved data reconstruction. During the tests two main events were recorded; the measurements (t_{ij}) and the beginning of a structure motion cycle (t_i). The measurement events were detected using the first laser pulse trigger signal. As far as the beginning of the structure motion cycle is concerned the swiveling period starting position was detected using an electronic angular position sensor.

After the acquisition of the time dependent measurements a specific software computed the period of each individual cycle (T_i) and the time-phase angle of each individual measurement within the correspondent structure cycle (t_j). Finally the resolved data was sorted in a reference structure motion period according to a desire time-phase resolution and accuracy.

3.3 Flow field measurements

Particle Image Velocimetry was the measuring technique chosen to measure the flow surrounding the flexible structure. The PIV system consisted of two 1280 pixel \times 1024 pixel synchronized cameras and a pulsed Nd:YAG laser with a wave length of 532 nm.

The two cameras were arranged in parallel to the structure rotating axel to visualize the flow in a plane perpendicular to it. To assure the correct position of the two adjacent images a special support was designed to hold both cameras and to permit the adjustment of each individual camera or both cameras simultaneously in the 6 spatial axis. The correspondent images acquired by the two cameras were stitched in the MatLab work space using a post-processing software before being cross-correlated.

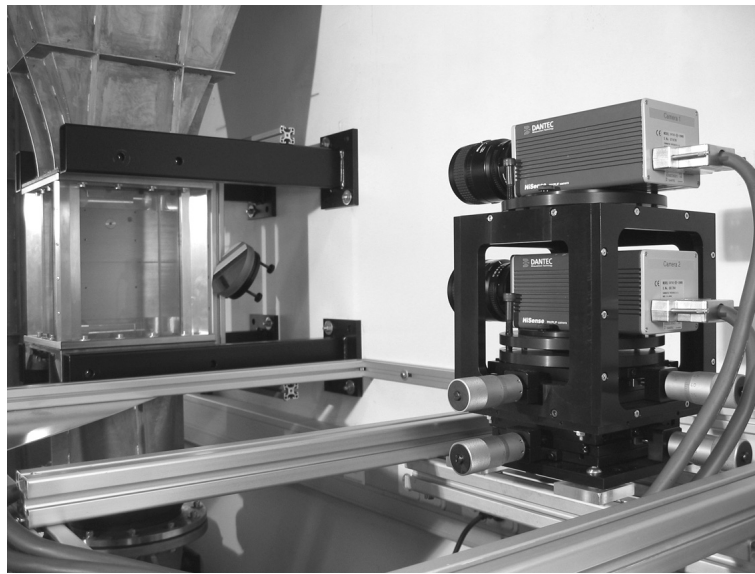


Fig. 5. Two-component PIV cameras and facility test section.

Two laser sources were used to illuminate the flow. This solution was adopted because the flexible structure was an opaque body which creates an unsteady dark shadow region in the fluid behind it when illuminated by just one light source. This behavior not only reduced the measuring area to almost one side of the flexible structure but also made the masking of the PIV images in post-processing difficult to be performed. Using one laser source to illuminate each side of the structure the dark region behind the structure was extinguished and all the flow surrounding the structure was accessible to PIV measurements. As a disadvantage it turned out that there were regions of different light intensity in the flow, however, this problem could be minimized with a proper adjustment of the laser light focus and cameras optics.

Opting for the solution of two parallel cameras and multiple light sources it was possible to acquire time-dependent composed PIV images at constant frequency of an extended 272 mm \times 170 mm flow field measuring area while keeping the spatial resolution as low as 133 μm \times 133 μm per CCD pixel.

As seeding particles 10 μm mean diameter silver coated hollow glass spheres were chosen. They reduce problems of light refraction and produce higher signal levels on high light absorbing media when compared with non-coated hollow glass spheres. The major drawback of using silver coated glass spheres is related to their density; the relative density of this kind of particles is about 1,4. Nevertheless, this drawback was accepted because of the high viscosity and the velocity of the flow during the test.

3.3 Structure deflection measurements

For structure deflection modes identification (DMI) measurements the PIV system was modified to provide it with structure deflection analysis capabilities. The idea behind this set-up was to use the PIV system to acquire and organize images from the swiveling structure and to use an especially developed software to analyze and reconstruct the time dependent deflection of the structure. The major advantage of this approach was that the same measuring system used for the velocity field measurements could be employed.

Only one camera was positioned to acquire images of the flexible structure illuminated by the laser sheet from each side of the model. After image acquisition, 3D PIV software including camera calibration routines that measure and account for perspective distortion were implemented to correct parallax errors and to compute the real scale of the structure deflection images.

The quantitative analysis was performed in Matlab workspace by a script developed for the specific task. The software analyzed and compared the PIV images with different illumination and reconstructed the time dependent image of the light sheet reflected by the structure. To achieve that purpose it mapped the pixel value in the grayscale of the entire image and detected the line resulting from the intersection of the laser sheet and the structure as well as the edges of the rear mass.

With the information of the position of the membrane and of the time-phase detector module the algorithm finally computed all the relevant time-phase resolved data about the structure movement such as, time-phase resolved angle of attack of the front body, structure deformation shape and coordinates of the structure trailing edge. Based on this data the modes present in the structure were identified and characterized.

4 EXPERIMENTAL RESULTS

The structure model was tested in a viscous liquid flow at different velocities up to 2 m/s. Figure 6 represents the behavior of the structure under consideration versus the velocity of the approaching fluid. The minimum velocity needed to excite the movement of the structure slightly varied from test to test. In most of the cases it was already possible to achieve a consistent swiveling motion for velocities slightly smaller than 1 m/s. From this point on the frequency of the structure movement increased linearly with the velocity of the approaching fluid. One important remark is related to the fact that as soon as a structure started swiveling its motion frequency coincide with the line of figure 6 independently of the velocity value at what the movement has started. The mode shift occurring showed a pronounced hysteresis

depending on increasing versus decreasing flow velocity.

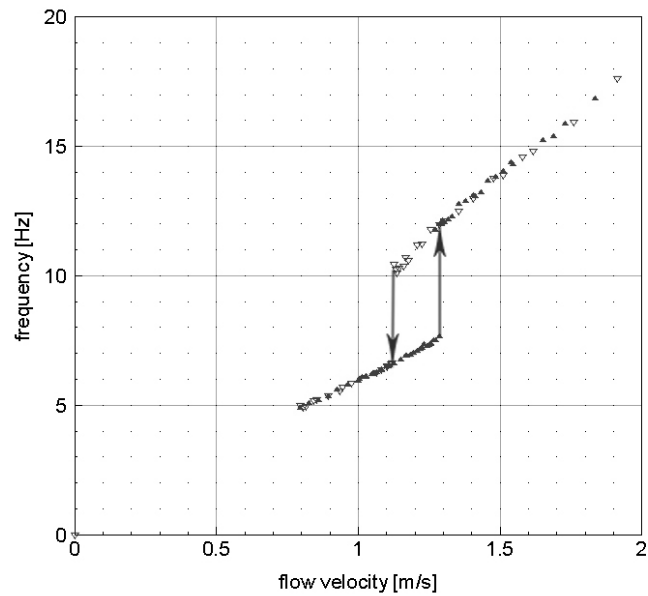


Fig. 6. Structure swiveling frequency versus incoming flow velocity (upward triangles correspond to measurements acquired while increasing velocity and downward ones while decreasing flow velocity).

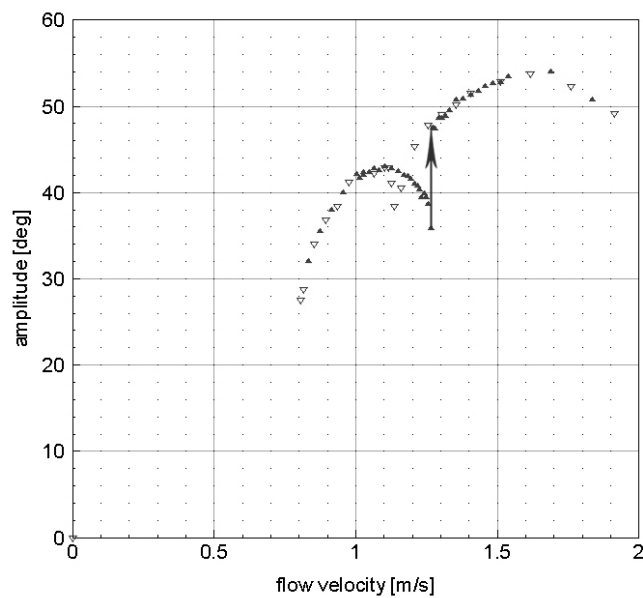


Fig. 7. Structure swiveling amplitude versus incoming flow velocity (upward triangles correspond to measurements acquired while increasing velocity and downward ones while decreasing flow velocity).

The swiveling motion mode shown by the structure at lower velocities was mostly characterized by its first deflection mode and by a frequency close to the first natural frequency of the structure (≈ 6 Hz). Figure 8 refers to a visualization performed at 1,08 m/s and it puts in evidence the first mode of the structure swiveling motion.

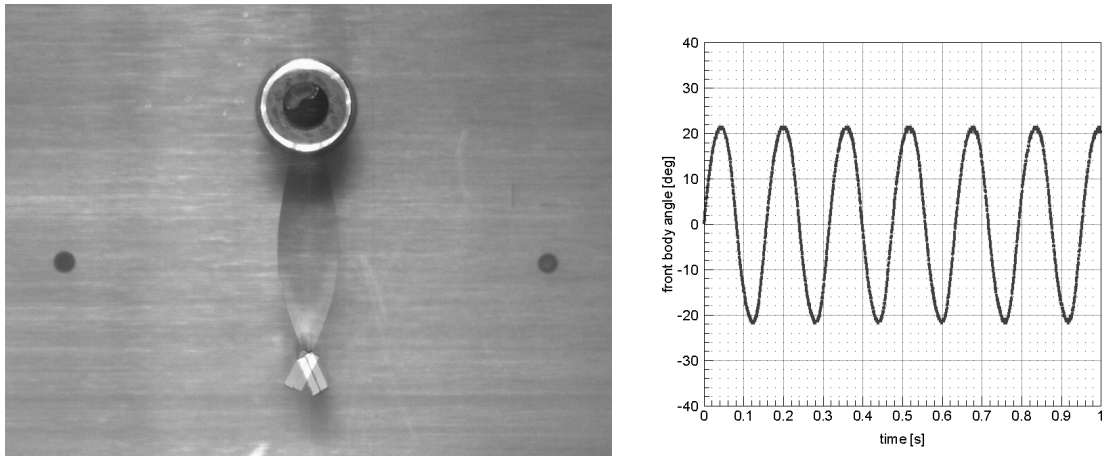


Fig. 8. Left: Superposition of images at a time-phase angle of 90° and 270° for an incoming velocity of 1,08 m/s. Right: Frequency of the structure swiveling motion for the same velocity.

At higher velocities the motion of the structure became faster and more complex. At around 1,3 m/s the structure shifted abruptly to a new swiveling mode in which the second deflection mode played an important role. A visualization performed at 1,45 m/s is presented in figure 9 and displays clearly the second swiveling mode.

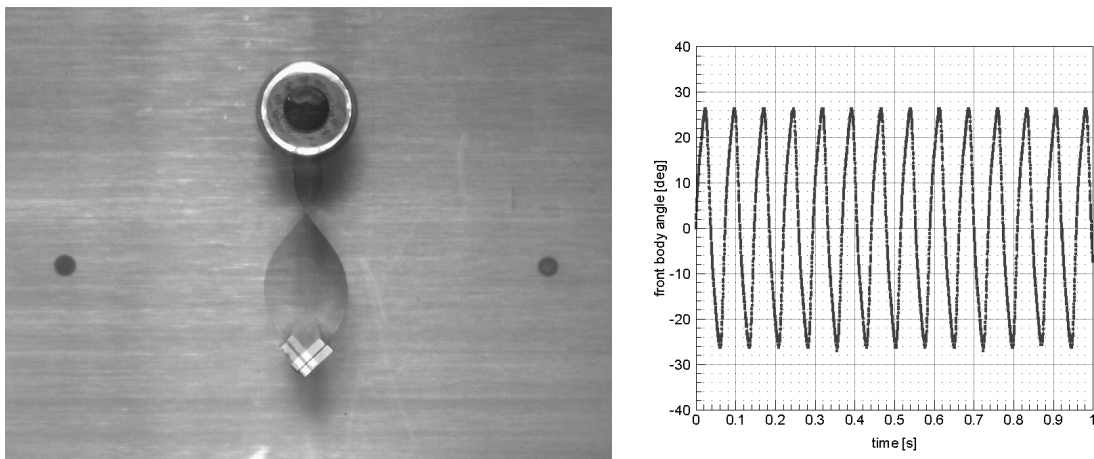


Fig. 9. Left: Superposition of images at a time-phase angle of 90° and 270° for an incoming velocity of 1,45 m/s. Right: Frequency of the structure swiveling motion for the same velocity.

In both motion modes the frequency of the structure increased linearly with the velocity of the fluid. Within the well defined velocity range from 1,1 m/s and 1,3 m/s the structure presented a hysteretic behavior where both swiveling modes could be observed depending on the previous frequency of the membrane.

The same hysteretic behavior between the two different swiveling modes can be observed when the amplitude of the structure movement is plotted versus the incoming flow velocity (see Fig. 7). The maximum amplitude for the first swiveling mode occurred around 1,1 m/s while for the second mode around 1,65 m/s.

After this first overview on the behavior of the structure tests were conducted at a constant incoming velocity of 1,45 m/s which corresponded to a Reynolds number, based on the diameter of the front cylinder, of 195. Figure 10 represents the test section inlet velocity profile measured at the location $x = -55$ mm in the absence of any model. It could be considered perfectly uniform except in the regions of the laminar boundary layers. The flow angularity was better than $0,5^\circ$ and the RMS of the velocity magnitude varied less than 1%.

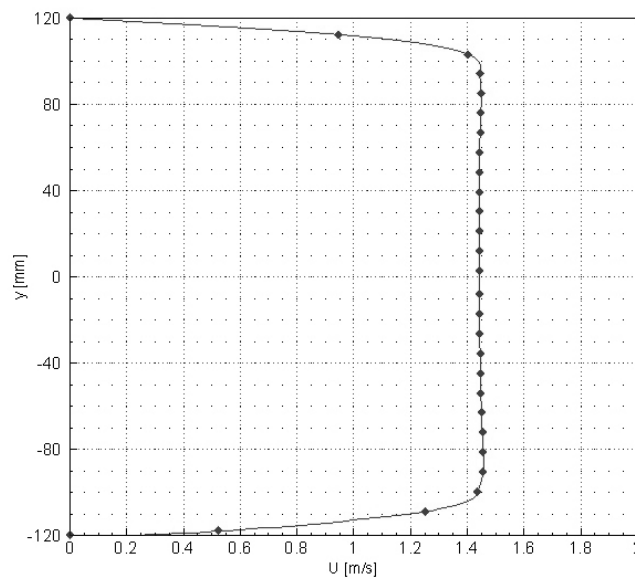


Fig. 10. Measured inlet velocity profile.

In figure 11 and 12 two global characteristic parameters of the response of the structure are represented: the front angle of attack and the coordinates of the trailing edge within the reference period of the structure periodical motion. The accuracy of the detection of the position of the structure was proven to be of the order of 0,3 mm.

As far as the evolution of the flow field is concerned figure 13 compiles the velocity field surrounding the structure at different instants of the reference swiveling period. The measurements were resolved in the time-phase space with an angle resolution of $2,5^\circ$ within an

uncertainty of $\pm 0,5^\circ$. The frequency of the swiveling motion of the structure at 1,45 m/s was measured to be 13,58 Hz with a maximum fluctuation from cycle-to-cycle of 2%.

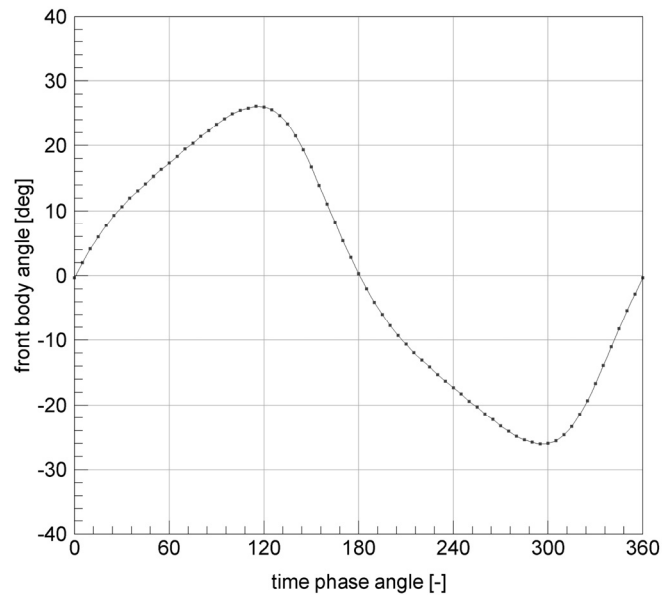


Fig. 11. Front body angle of attack within the reference period of motion.

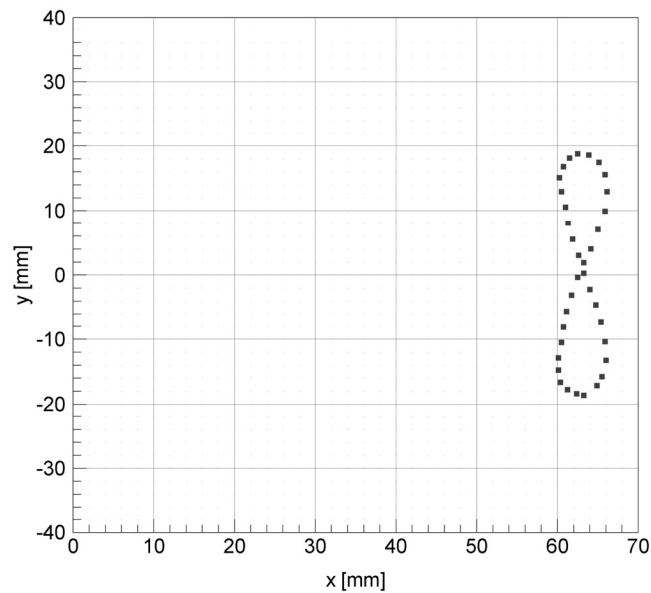
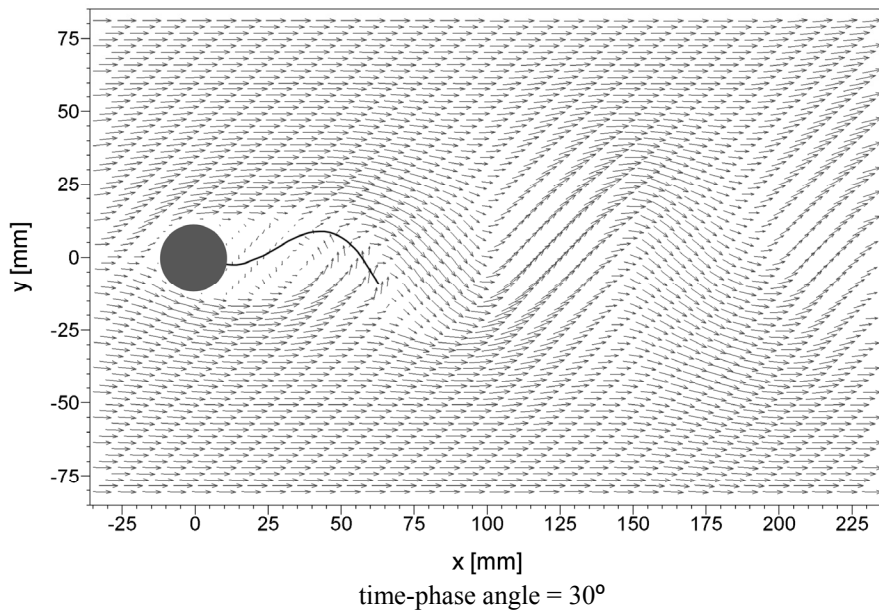
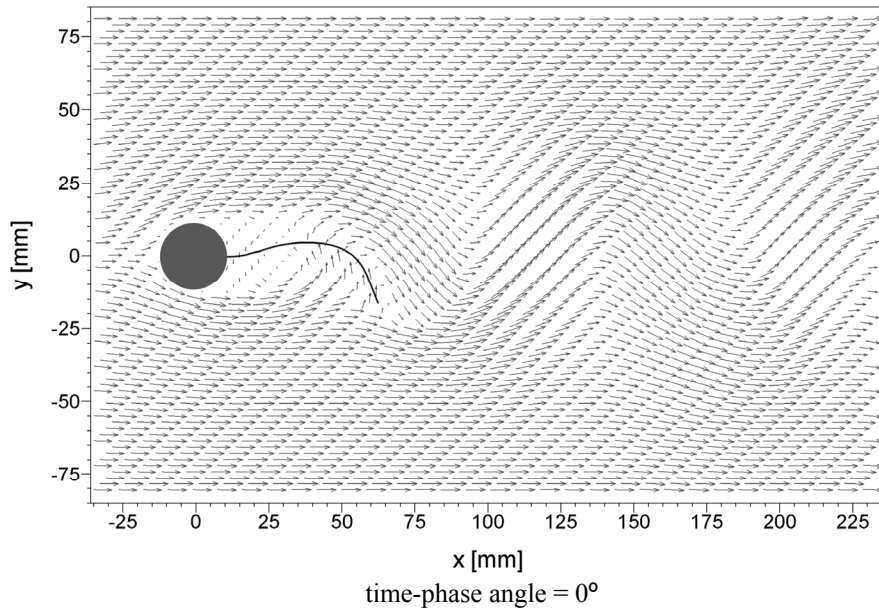
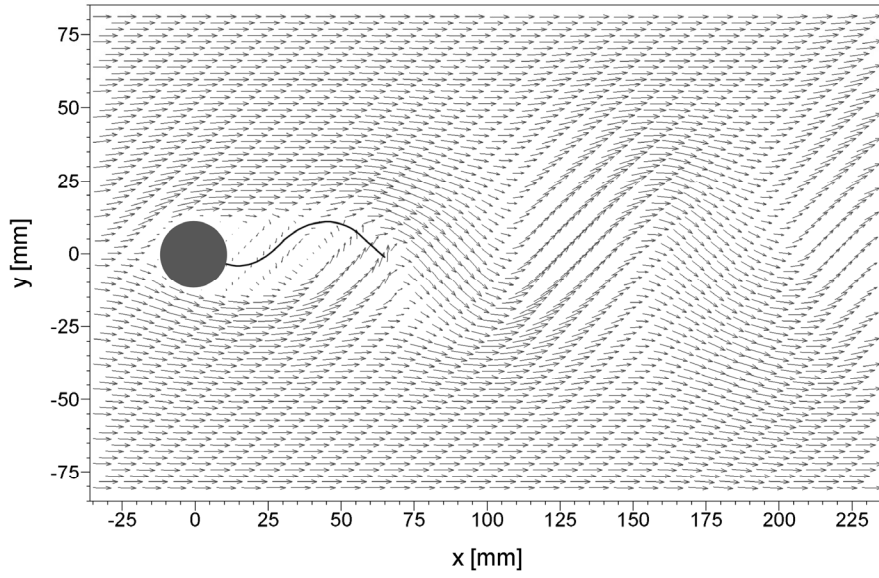


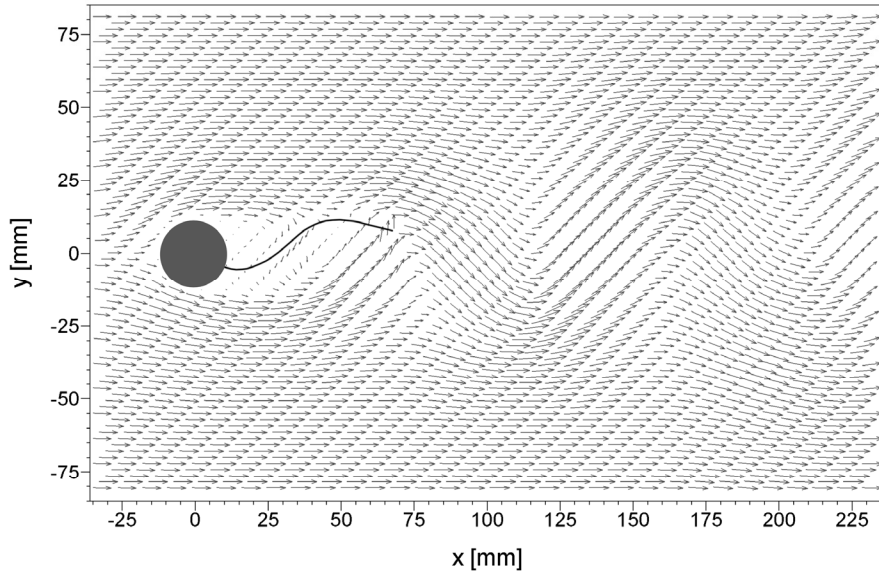
Fig. 12. Coordinates of the structure trailing edge within the reference period of motion.

Each velocity field corresponds to the average value of 100 maps acquired for the same time-phase angle. The flow field measurements cover a flow area from $(x,y)=(-36\text{ mm},-85\text{ mm})$ to $(x,y)=(236\text{ mm},85\text{ mm})$. Comparing the velocity fields with figure 11 one can conclude that in the firsts 4 maps the front body it is rotating clockwise while in the last ones is rotating in the opposite direction. At 120° the angular velocity of the front body is almost zero.





time-phase angle = 60°



time-phase angle = 90°

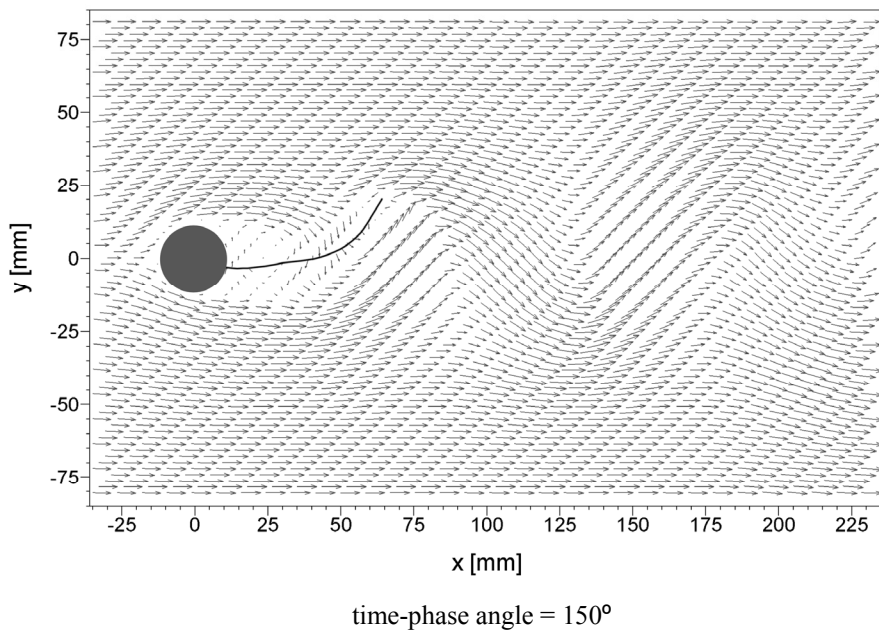
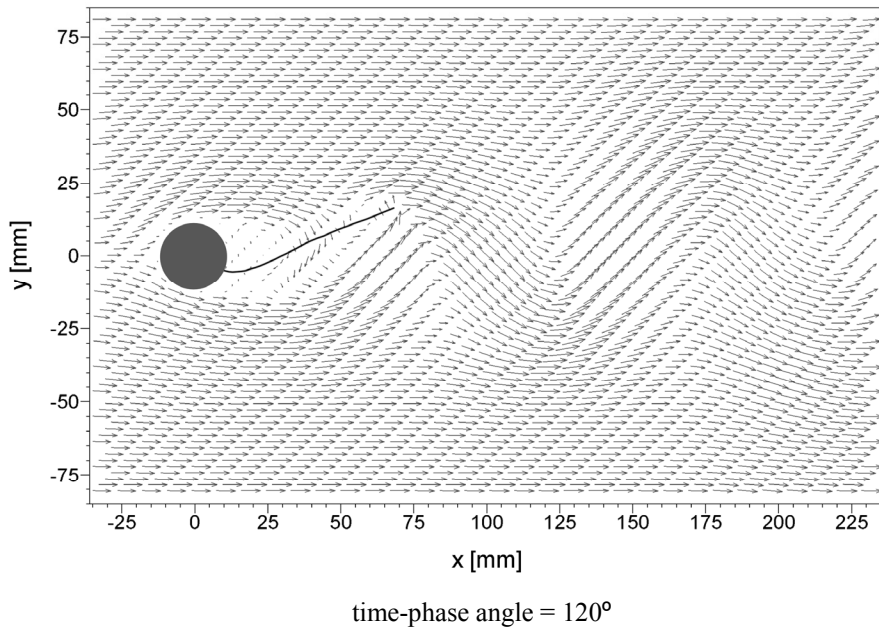


Fig. 13. Time-phase resolved combined velocity flow field / structure deflection results at six different instants on the reference swiveling motion period.

5 CONCLUSIONS

The increased efforts in numerical research to develop coupling strategies for the simulation of fluid-structure interaction problems have triggered the development of a reference experiment on the same research field.

Within this work, a new test facility was constructed to perform tests with laminar and turbulent flows. The dedicated tunnel was designed to be operated with fluids of different viscosities and has satisfied all the design objectives. It permits to perform the tests under very precise boundary and working conditions both with water or high viscous liquids (with a kinematic viscosity up to $5 \times 10^{-4} \text{ m}^2/\text{s}$).

As far as the measurement techniques are concerned Particle Image Velocimetry was successfully applied to measure the velocity of the flow surrounding the flexible structure and, with some modifications, to measure the deflection of the structure. The insertion of the time-phase detector module made the reconstruction of the unsteady periodic time-phase resolved measurements reliable and extremely accurate. Because of its architecture, this approach has turned out to be more memory consuming compared to other solutions but yielded accurate time-phase resolved measurements reconstruction independently from the nature of the structure motion.

In this paper results are presented that were obtained for a bluff front body flexible structure in laminar flow. The structure was constituted by a thin metal sheet attached to a front cylindrical free rotating body. At the trailing edge of the metal sheet a rear mass was attached. The reference structure model has proven to fulfill all the requirements needed, in special it showed a very reproducible symmetrical two-dimensional swiveling motion.

About the dynamic response of the structure it evidenced two distinctive modes of vibration depending on the approaching flow velocity. The two different modes are separated by a hysteretic region in which both modes could be observed for the same test conditions. This behavior is in agreement with the galloping response of square cross-section prisms as reported by Parkinson³ and Novak⁴. For both swiveling modes the frequency of the structure motion increased with the fluid velocity. Regarding the vibration amplitude the structure presented two local maximum, one for each mode of vibration. The first maximum was situated at around 1,1 m/s while the second was noticed for about 1,65 m/s.

A detailed characterization of the self-excited coupled unsteady flow and structure motion driven by a uniform incoming flow at 1,46 m/s was presented. The frequency of the structure at this velocity was measured to be 13,58 Hz with a maximum deflection of the front body of $\pm 26^\circ$. A data base was compiled on the flow velocity field around the structure as well as on the deflection of the structure within the reference swiveling period. The time-phase data was reconstructed with a resolution of $2,5^\circ$ and it is now available and constitute a useful tool for validation and comparison of different numerical simulations. From this data base results for six specific time-phase angles are shown in this paper.

6 ACKNOWLEDGEMENTS

The present study was part of a research project of the DFG Forschergruppe 493 - Fluid-Struktur-Wechselwirkung: Modellierung, Simulation, Optimierung. The authors gratefully acknowledge the financial support for their research work through the German Science Foundation (DFG) - Germany and Fundação para a Ciência e a Tecnologia (FCT) – Portugal.

REFERENCES

- [1] E. Naudasher and D. Rockwell, *Practical experiences with flow-induced vibrations*, Springer (1980).
- [2] E. Naudasher and D. Rockwell, *Flow-induced vibrations – An engineering guide*. A.A. Balkema (1994).
- [3] G.V. Parkinson and J.D. Smith, “The square prim as an aeroelastic non-linear oscillator”, *Quarterly, Journal of Mechanics and Applied Mathematics*, **17**, 225-239 (1964).
- [4] M. Novak, “Galloping oscillator of prismatic structures”, *Journal of the Engineering Mechanics Division*, **98**, 27-46 (1972).